

Fault Detection Method by Utilizing Instantaneous Power Theory for Inverter-based Distributed Generation

Nattapat Praisuwana, Leon M. Tolbert, Jingxin Wang, and Fangxing Li
Min H. Kao Department of Electrical Engineering and Computer Science
The University of Tennessee, Knoxville, TN, USA
npraisu1@vols.utk.edu

Abstract— The integration of distributed generation (DG) into electric grid systems results in some significant consequences for the protection of distributed systems. Distributed systems that have high penetration of inverter-based distributed generation (IDG) will have changes in fault current levels causing traditional overcurrent protective devices to not operate as intended. As a result, distributed systems require new protection schemes to deal with the wide varieties of IDG, which need significant investment in the protection devices. This paper discusses the impact of IDGs on the protection of the distributed system. To solve the issues faced in grids with IDG, a fault detection method that utilizes instantaneous power theory is proposed. Simulation and experimental results illustrate how this theory can be used to detect faults even with low fault current levels.

Keywords—Fault detection, instantaneous power theory, low fault current, active power, nonactive power, inverter-based distributed generation.

I. INTRODUCTION

As worldwide electricity demand rapidly increases, renewable energy sources (RESs) such as wind and photovoltaics are two of the solutions to provide more environmental friendly generation. The increasing use of RESs in distribution networks benefits overall power grids by reducing the need for the construction of new transmission lines, reducing system losses, and increasing the resiliency of distribution networks. Most RESs are interfaced to the distribution networks by inverters, so called inverter-based distributed generation (IDG) while most conventional generation comes from synchronous generators [1].

Conventional generators such as nuclear and coal power plants require transmission lines to transfer power from the generation to load because they are located far away from loads as shown in Fig. 1. On the other hand, the future power network with microgrids requires less transmission lines because microgrids are a group of loads and generators in defined boundaries as shown in Fig. 2. Also, microgrids have the ability to integrate DGs and IDGs into the system directly [1]-[3].

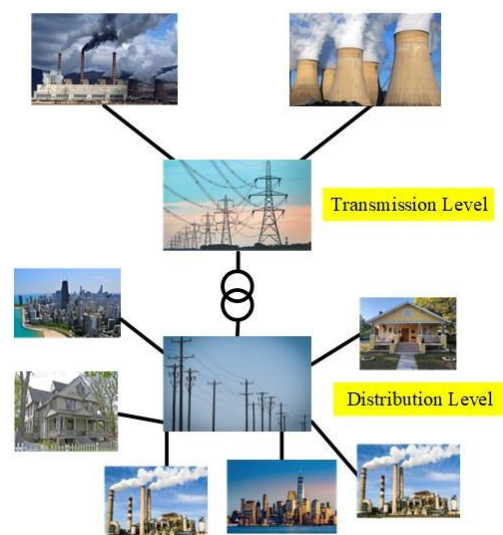


Fig. 1. Conventional power network [2].

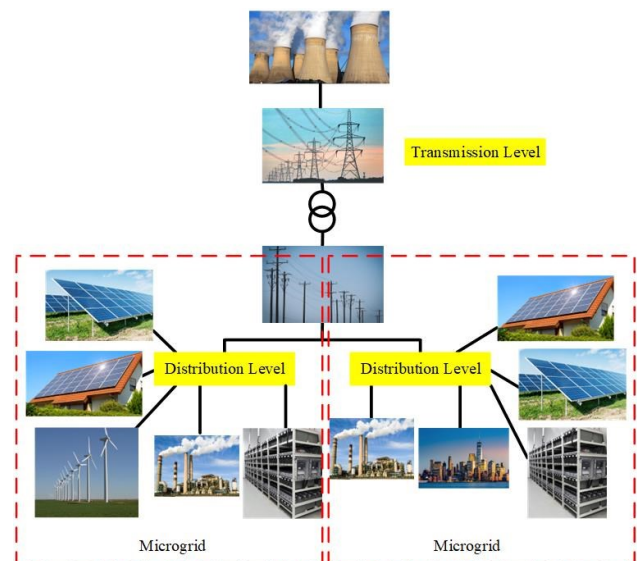


Fig. 2. Future power network consisting of microgrids [2].

However, the more IDGs that connect to distribution networks, the more complex these networks will be. One of the challenges for a distribution protection system is the changing fault current levels. Because conventional power networks are not typically operated in the islanded mode, the fault current levels do not change much. On the other hand, IDGs are able to operate in both grid connected mode and islanded mode, and these different operation regimes also have an effect on fault current levels. That is the reason why protective devices may not function as intended since the fault current levels are quite different between grid-connected and islanded modes [2] - [6].

Thus, this paper presents a fault detection method by utilizing instantaneous power theory to allow power converters to be able to identify the faults. This fault detection method is also proposed to improve the protection system for inverter-based distribution networks with modified fault current level. This paper is organized as follows: Section II provides instantaneous power theory. Section III explains a proposed fault detection method. Section IV presents simulation details. Section V illustrates experimental results. Section VI provides the conclusion.

II. INSTANTANEOUS POWER THEORY

Instantaneous power theory has been applied to several applications. It has been used to do THD estimation for smart power meters [7]. The concept is to calculate instantaneous active power and reactive power. Then, the fundamental and harmonic components can be obtained. Another application is for a shunt compensator for nonactive (reactive) power. A definition of nonactive current has been presented, and instantaneous active and nonactive power were derived to compensate for both periodic and non-periodic currents [8] - [10].

For a three-phase system, the total instantaneous power is the sum of the active powers of each of the individual phases as shown in (1).

$$p(t) = \sum_{k=1}^3 p_k(t) = \sum_{k=1}^3 v_k(t) i_k(t) \quad (1)$$

Active and nonactive power definition [8] is used to obtain instantaneous active and non-active power in this paper. Nonactive power is the power circulating in the system either

between a source and loads or between phases. The instantaneous active current $i_a(t)$ and nonactive current $i_n(t)$ are

$$i_a(t) = \frac{P_a(t)}{V_P^2(t)} v_P(t), \quad i_n(t) = i(t) - i_a(t) \quad (2)$$

where $P_a(t)$ is the average active power, $v_P(t)$ is the reference voltage, and $V_P(t)$ is the rms value of $v_P(t)$.

$$P_a(t) = \frac{1}{T_c} \int_{t-T_c}^t p(\tau) d\tau = \frac{1}{T_c} \int_{t-T_c}^t v(\tau) i_a(\tau) d\tau \quad (3)$$

$$V_P(t) = \sqrt{\frac{1}{T_c} \int_{t-T_c}^t v_P^2 d\tau}, \quad (4)$$

The average nonactive power $P_n(t)$ is defined as (5).

$$P_n(t) = \frac{1}{T_c} \int_{t-T_c}^t v(\tau) i_n(\tau) d\tau \quad (5)$$

To obtain the instantaneous active and nonactive power, T_c is set to zero. This instantaneous power theory is utilized in a proposed fault detection method, illustrated in the next section.

III. PROPOSED FAULT DETECTION METHOD

The instantaneous power theory including active power and nonactive power is utilized in a proposed fault detection method. The proposed fault detection method needs inverter output voltage and current which are already provided for inverter control purposes. Therefore, no additional measurement device is required for this proposed fault detection method.

The proposed fault detection method is illustrated in Fig. 3. Inverter output current and voltage are inputs to perform instantaneous power calculations continuously to ensure that they are in a normal condition within thresholds shown in Table I. If the active and nonactive power exceed these thresholds, then current and voltage shown in Table I are checked. If both voltage is outside the range 0.88 – 1.1 pu and current exceeds the threshold which is 1.2 pu., then a fault signal will be triggered.

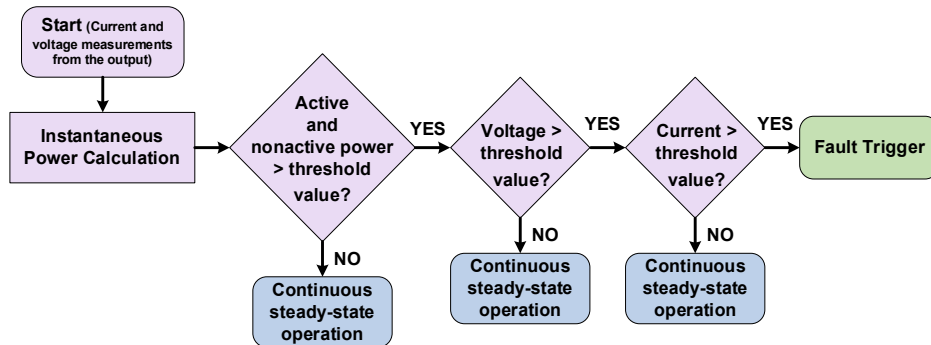
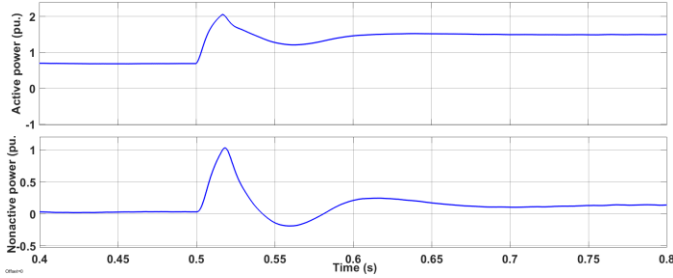


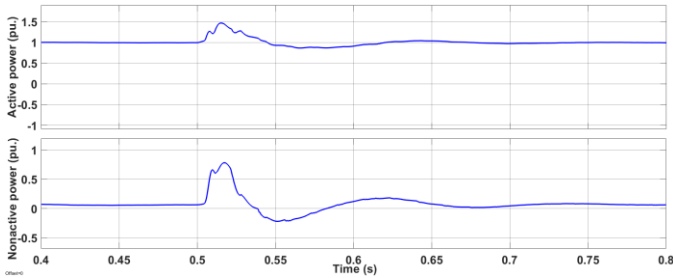
Fig. 3. Proposed fault detection method using instantaneous power.

TABLE I. THRESHOLD SETTINGS

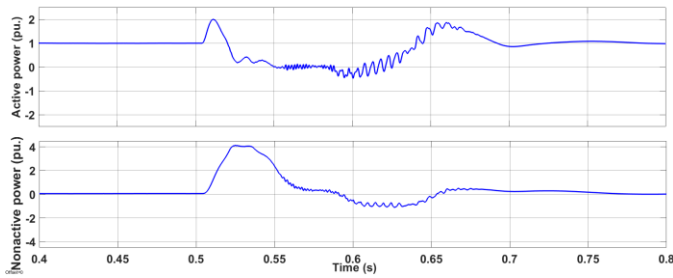
| Threshold | Value (pu.) |
|-----------------|-------------|
| Voltage | 0.88 – 1.1 |
| Current | 1.2 |
| Active power | 1.5 |
| Nonactive power | 2.5 |



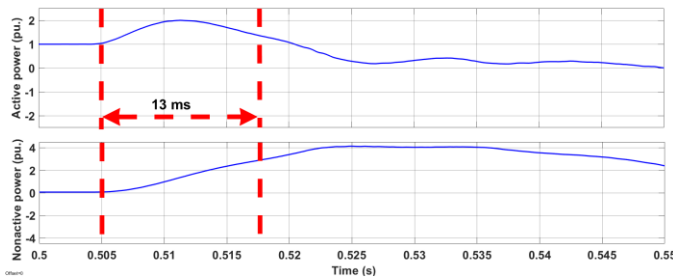
(a)



(b)



(c)



(d)

Fig. 4. Instantaneous active power and nonactive power waveforms for several events: (a) motor start; (b) transformer energization; (c) fault event; (d) zoomed in fault event.

The voltage threshold in Table I is referred from IEEE 1547-2018 [11]. When the voltage level is within the range 0.88 – 1.1 pu, IDGs are required to continuously operate. To protect power switches in IDGs from high currents, the current threshold is set at 1.2 pu. To avoid unnecessary tripping, several transient conditions including motor starting and transformer energizing are considered. Fig. 4 shows instantaneous active power and nonactive power for each event. Motor starting event shown in Fig. 4(a) and transformer energizing event shown in Fig. 4(b) happen at 0.5 s, and a fault event shown in Fig. 4(c) is at 0.5042 s. Starting a motor and energizing a transformer have similar behaviors in both active and nonactive power. Active power for starting motor is 2 pu. and nonactive power is 1 pu. For transformer energization, active power is 1.5 pu and nonactive power is around 0.75 pu. When examining these three different events, a fault condition consumes the largest nonactive power, approximately 4 pu.

Although a fault condition has distinct behavior, active power and nonactive power thresholds need to be optimized. If the thresholds of the power are too high, the fault detection and operation time will be too long or protective devices may not even operate. On the other hand, if the thresholds are too low, unnecessary tripping may happen since it may detect the other transients as a fault.

Also, each system may have different fault behaviors such as fault current capacity and fault current waveform, so instantaneous power calculation during faults in the system needs to be studied in order to optimize the power thresholds. It is similar to power flow study for protection relay setting. So, for these studied systems shown in Fig. 5 and 10, the threshold of active power is 1.5 pu and nonactive power is 2.5 pu.

However, since during the fault, a rate of increasing of nonactive power is slower than active power as shown in Fig. 4(d), the active power value needs to exceed the threshold for a half cycle (8 ms). When active and nonactive powers exceed the threshold, fault detection will be triggered immediately. As a result, this proposed fault detection method has been optimized, and it is ready to be implemented in IDGs.

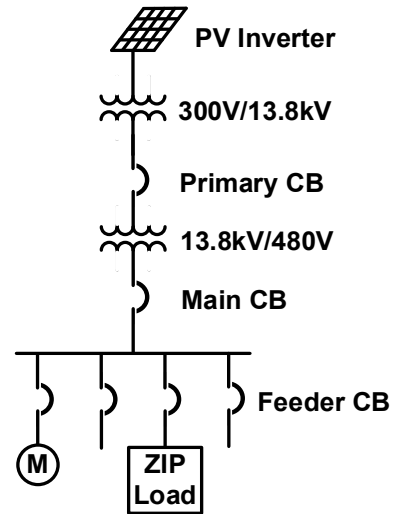


Fig. 5. Studied microgrid system with IDG.

IV. SIMULATION

The proposed fault detection method has been implemented in an IDG, PV inverter, in a studied system illustrated in Fig. 5. The system includes circuit breakers, transformers, and loads, so it can be used to study transient and fault conditions and associated protection. Fig. 6 shows the fault detection method can successfully detect a fault in the system in 13 ms because active power and nonactive power are calculated in real time. Therefore, this proposed fault detection method is acceptable in accuracy and sensitivity.

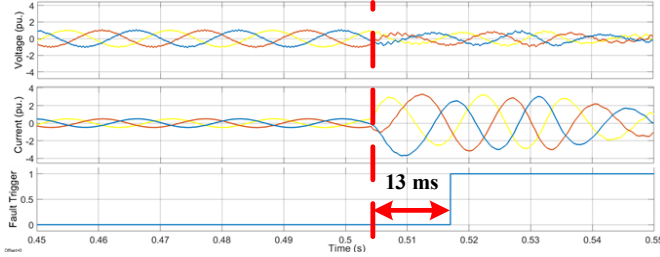


Fig. 6. Performance of the proposed fault detection method.

V. EXPERIMENTAL RESULTS

This proposed fault detection method has been tested in a power converter-based hardware test bed (HTB) shown in Fig. 7. The HTB is a power grid emulator which can emulate both transmission and distribution networks. The HTB consists of power converters to emulate various loads, generator, RESs, and energy storage in a power grid [12], [13]. The HTB also has the capability of fault emulation [14], [15]. The proposed fault method has been experimentally tested in two microgrid systems. First is a simple microgrid shown in Fig. 5 to test the concept of instantaneous power calculation. Then, a more complex microgrid shown in Fig. 10 is to demonstrate fault detection performance.

A. Simple Microgrid System with IDGs

First, a 3-phase fault has been emulated in a studied microgrid system shown in Fig. 5 to test the proposed fault detection method. Fault emulation in the studied microgrid is shown in Fig. 8. The proposed fault detection method has been implemented in the controller DSP of power inverters. Fig. 9 illustrates an experimental result of real-time active and nonactive power calculation by the DSP. Then, a fault signal will be triggered if these values exceed the thresholds.

B. Banshee Microgrid

To further verify performance of the fault detection method, Banshee microgrid [16] has been chosen to be a demonstrated system. Fig. 10 illustrates a simplified Banshee microgrid. The microgrid consists of generators, RESs, a motor load and ZIP loads. A microgrid control center screen using LabVIEW is shown in Fig. 11. A left column on the screen is switches to turn on and off sources and loads. Power consumption of loads and power output of sources can be controlled by changing numbers in a middle column on the screen. The right column on the screen is a ramp rate for loads and sources.

Also, active power, nonactive power, voltage, and frequency of loads and sources are monitored on the right of the screen. The top graph shows an instantaneous active power. The lower graph is an instantaneous nonactive power. The third graph monitors voltage, and frequency is displayed in the bottom graph. When it shows the proposed fault method is able to detect a fault, the fault indicator on the screen will turn to red.



Fig. 7. Power converter-based hardware test bed (HTB).

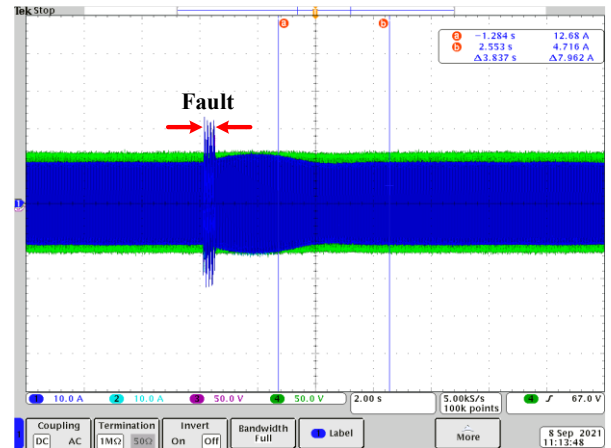


Fig. 8. Fault emulation in HTB.

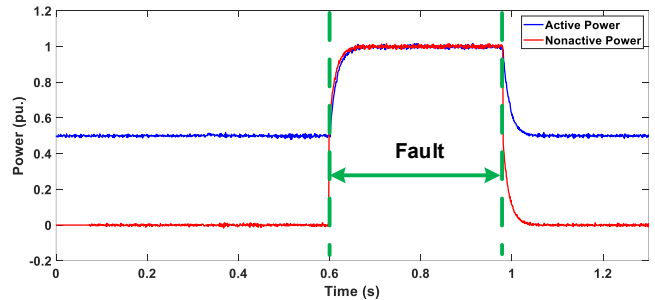


Fig. 9. Active and nonactive power calculation.

Three-phase faults have been emulated for 100 ms at different buses in the microgrid to test a fault detection function of IDGs including PV and BESS. Both IDGs have the same control scheme (grid following) and the current limit is set at 2 pu. Fig. 12 demonstrates real-time active and nonactive power calculation and fault detection of PV and BESS inverters when a fault occurs at BUS 101. It can be seen that PV and BESS inverters have similar instantaneous power outputs due to the same control scheme and since the values exceed the threshold in Table I, both of them are able to detect the fault within 12 ms and 13 ms, respectively.

Also, the fault detection method has been tested with all possible fault locations in the microgrid system including BUS 102, 105 and 106, while BUS 103 is normally open, a green box. So, a fault at BUS 103 has not been tested. Due to similarity of PV and BESS instantaneous power outputs, only BESS outputs will be illustrated. Hence, Figs. 13, 14, and 15 show BESS instantaneous power outputs and fault detection when BUS 102, 105 and 106 are faulted, respectively.

Fig. 13 illustrates instantaneous power outputs and fault detection of BESS during a fault at BUS 102. BESS is able to detect the fault in 12 ms. Once a fault happens at BUS 105, instantaneous power outputs and fault detection of BESS is shown in Fig 14, and the fault can be detected in 13 ms. Fig. 15 demonstrates BESS instantaneous power outputs and fault detection once a fault occurs at BUS 106. This fault can be detected slower than the other cases which is 14 ms. However, all faults can be identified within less than 1 cycle (16 ms) which is much faster than traditional overcurrent relays (≈ 50 ms).

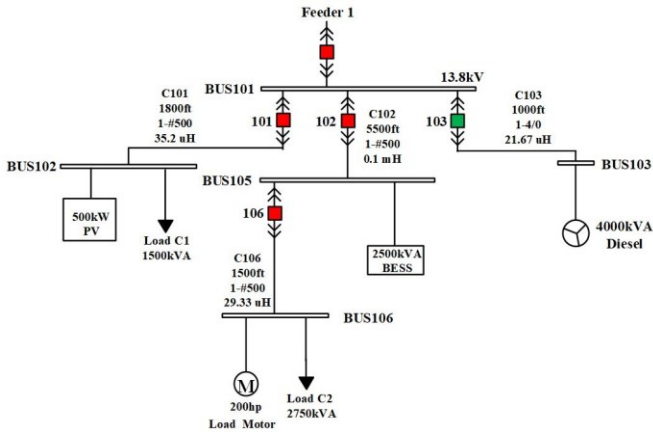


Fig. 10. Simplified Banshee microgrid.

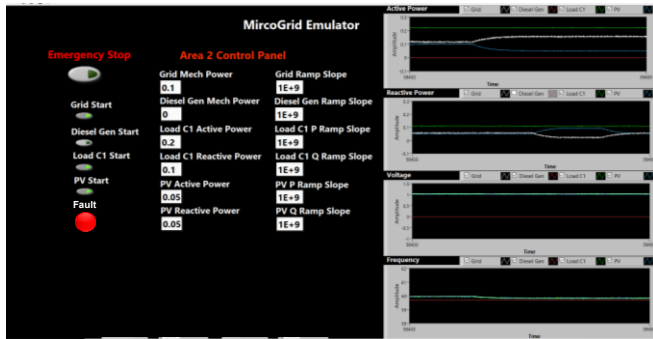
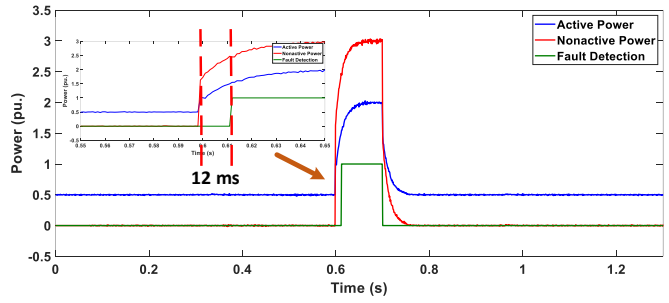
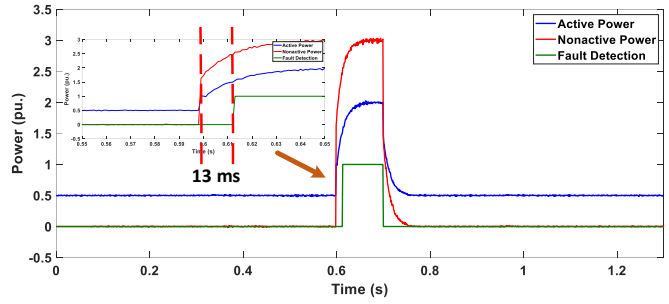


Fig. 11. Control center screen for microgrid emulator.



(a)



(b)

Fig. 12. Instantaneous power calculation and fault detection for a fault at BUS 101: (a) PV; (b) BESS.

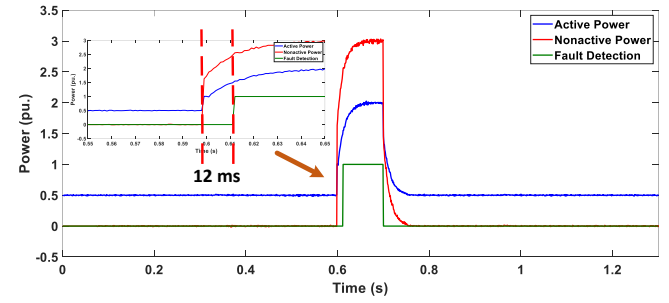


Fig. 13. BESS instantaneous power calculation and fault detection for a fault at BUS 102.

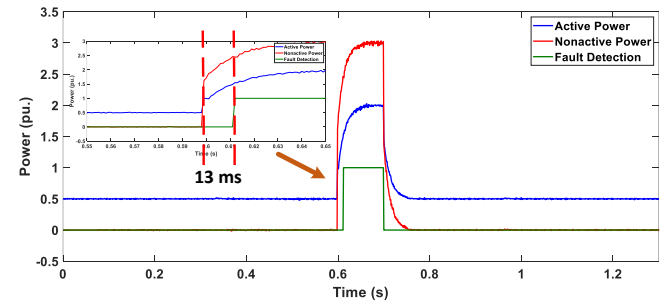


Fig. 14. BESS instantaneous power calculation and fault detection for a fault at BUS 105.

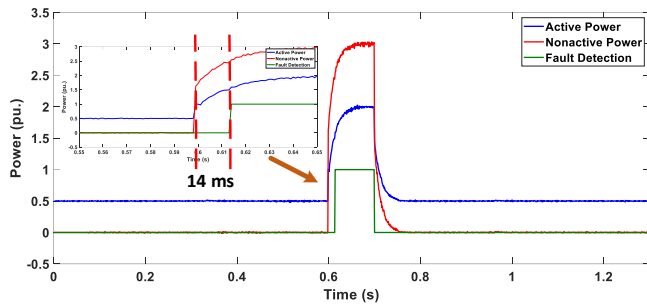


Fig. 15. BESS instantaneous power calculation and fault detection for a fault at BUS 106.

VI. CONCLUSION

To improve inverter-based distribution protection systems, this paper proposes a new fault detection method by utilizing instantaneous power theory. Instantaneous power calculation including active power and nonactive power is presented in this paper. Furthermore, by utilizing instantaneous active power and nonactive power calculation and optimizing the thresholds, simulation results shows that the proposed fault detection method can identify faults quickly and accurately. Experimental results illustrate that instantaneous active and nonactive power calculations have been implemented in the controller DSP of power converters, and it has been tested in the HTB. The proposed fault detection method successfully identified all fault events in the Banshee microgrid. Therefore, this proposed fault detection method is reliable and effective for IDGs in microgrid systems.

ACKNOWLEDGMENT

This research is supported by supported by the Engineering Research Center Program of the National Science Foundation and DOE under NSF Award Number EEC-1041877.

REFERENCES

- [1] F. Blaabjerg, Y. Yang, D. Yang and X. Wang, "Distributed power-generation systems and protection," *Proceedings of the IEEE*, vol. 105, no. 7, pp. 1311-1331, Jul 2017.
- [2] B. Kroposki, B. Johnson, Y. Zhang, V. Gevorgian, P. Denholm, B. M. Hodge, and B. Hannegan, "Achieving a 100% renewable grid: operating electric power systems with extremely high levels of variable renewable energy," *IEEE Power Energy Mag.*, vol. 15, no. 2, pp. 61-73, Mar./Apr. 2017.

- [3] The U.S. Department of Energy (DOE) Office of Electricity Delivery and Energy Reliability (OE), *Microgrid workshop report*, Aug. 2011. [Online]. Available: <https://www.energy.gov/oe/downloads/microgrid-workshop-report-august-2011>.
- [4] M. A. Zamani, T. S. Sidhu, and A. Yazdani, "A protection strategy and microprocessor-based relay for low-voltage microgrids," *IEEE Trans. Power Del.*, vol. 26, no. 3, pp. 1873-1883, Jul. 2011.
- [5] B. Hussain, S. M. Sharkh, S. Hussain, and M. A. Abusara, "Integration of distributed generation into the grid: protection challenges and solutions," *10th IET International Conference on Developments in Power System Protection (DPSP 2010)*, pp. 1-5, Mar 2010.
- [6] F. Coffele, C. Booth, and A. Dysko, "An adaptive overcurrent protection scheme for distribution networks," *IEEE Trans. Power Del.*, vol. 30, no. 2, pp. 561-568, Apr. 2015.
- [7] L. Wang, C. Lam, M. Wong, "Total harmonic distortion (THD) estimation technique based on power concept for smart power meters," *IEEE PES Asia-Pacific Power and Energy Engineering Conference*, pp. 1-6, Dec 2019.
- [8] Y. Xu, L. M. Tolbert, F. Z. Peng, J. N. Chiasson, and J. Chen, "Compensation-based non-active power definition," *IEEE Power Electronics Letters*, vol. 1, no. 2, pp. 45-50, Jun 2003.
- [9] F. Z. Peng, L. M. Tolbert, and Z. Qian, "Definitions and compensation of nonactive current in power systems," in *IEEE Power Elect. Specialists Conference*, pp. 1779-1784, Jun 2002.
- [10] L. M. Tolbert, Y. Xu, J. Chen, F. Z. Peng, and J. N. Chiasson, "Application of compensators for nonperiodic currents," *IEEE Power Elect. Specialists Conference*, pp. 1525-1530, Jun 2003.
- [11] *IEEE Standard for Interconnection and Interoperability of Distributed Energy Resources with Associated Electric Power Systems Interfaces*, IEEE 1547, 2018.
- [12] J. Wang, L. Yang, Y. Ma, J. Wang, L. M. Tolbert, F. Wang, and K. Tomsovic, "Static and dynamic power system load emulation in converter-based reconfigurable power grid emulation," *IEEE Energy Conversion Congress and Exposition (ECCE)*, Sep. 2014, pp. 4008-4015.
- [13] L. M. Tolbert, F. Wang, K. Tomsovic, K. Sun, J. Wang, Y. Ma, and Y. Liu, "Reconfigurable real-time power grid emulator for systems with high penetration of renewables," *IEEE Open Access Journal of Power and Energy*, vol. 7, pp. 489-500, Nov 2020.
- [14] Y. Ma, L. Yang, J. Wang, F. Wang, and L. M. Tolbert, "Full-converter wind turbine emulator in converter based power grid emulation system," *IEEE Applied Power Electronics Conference and Exposition (APEC)*, Mar. 2014, pp. 3042-3047.
- [15] S. Zhang, B. Liu, S. Zheng, Y. Ma, F. Wang, L. M. Tolbert, "Three-phase short-circuit fault implementation in converter based transmission line emulator," *IEEE Energy Conversion Congress and Exposition (ECCE)*, Oct. 2017, pp. 2914-2920.
- [16] RTDS Technologies, "Banshee microgrid sample case," Nov 2019.